

Synthesis and Properties of Heterocyclic Substituted 1,2-Enedithiolates of Nickel, Palladium, and Platinum

Sharada P. Kaiwar,[†] John K. Hsu,[†] Louise M. Liable-Sands,[‡] Arnold L. Rheingold,[‡] and Robert S. Pilato^{*,†}

Department of Chemistry and Biochemistry, University of Maryland, College Park, Maryland 20742, and Department of Chemistry, University of Delaware, Newark, Delaware 19711

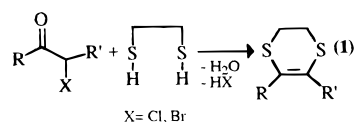
Received February 20, 1997[⊗]

A convenient new synthetic route to metallo-1,2-enedithiolates was applied to the synthesis of (dppe)M{S₂C₂-(heterocycle)(H)}; dppe = 1,2-bis(diphenyldiphosphino)ethane, M = Ni, Pd, and Pt, and heterocycle = 2-quinoxaline, 2-, 3-, and 4-pyridine, and 2-pyrazine. These complexes were prepared from the corresponding bis(hydrosulfido) complexes (dppe)M(SH)₂ and the α -bromo ketones, heterocycle-C(O)CH₂Br. In the solid state, (dppe)Ni{S₂C₂(2-pyrazine)(H)} is a slightly distorted square plane with a planar five-membered metallo-1,2-enedithiolate ring. The metallo-1,2-dithiolate is $\approx 6^\circ$ from being coplanar with the pyrazine ring. These complexes all have a UV-visible band assignable to an intraligand transition (ILCT) that is best described as a 1,2-enedithiolate $\pi \rightarrow$ heterocycle π^* charge transfer transition. The energy of the ILCT transition tracks with the reduction potential of the appended aromatic heterocycle. The pK_a of the protonated complexes is 1–3 units higher than that of the parent heterocycle, independent of the metal, and consistent with resonance stabilization of the protonated heterocycle by the 1,2-enedithiolate ligand.

Introduction

Considerable research has focused on the synthesis, reactivity, and physical and photophysical properties of metallo-1,2-enedithiolates.^{1–16} These complexes are of interest as components in magnetic^{5,6} and conducting^{3,7,8} materials, as models for the molybdenum cofactor (Moco),^{9–13} and as solution lumiphores.^{1,14–16}

In a previous study,¹⁷ a new synthetic route to metallo-1,2-enedithiolates, patterned after the synthesis of organic 1,4-dithiols^{18–20} (eq 1), was applied to the synthesis of a range of Cp₂Mo{S₂C₂(R)(R')} derivatives. This paper describes the



[†] University of Maryland.

[‡] University of Delaware.

[⊗] Abstract published in *Advance ACS Abstracts*, August 15, 1997.

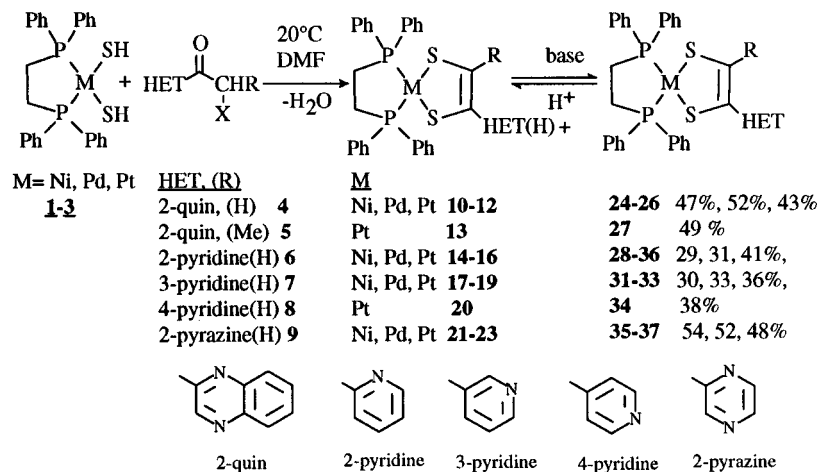
- Zuleta, J. A.; Burberry, M. S.; Eisenberg, R. *Coord. Chem. Rev.* **1990**, *97*, 47–64.
- Pilato, R. S.; Stiefel, E. I. *Catalysis by Molybdenum-Cofactor Enzymes*. In *Bioinorganic Catalysis*; Reedijk, J., Ed.; Marcel Dekker Inc.: New York, 1993; pp 133–88.
- (a) Cassoux, P.; Valade, L.; Kobayashi, H.; Kobayashi, A.; Clark, R. A.; Underhill, A. E. *Coord. Chem. Rev.* **1991**, *110*, 115–60. (b) Olk, R. M.; Olk, B.; Dietzch, W.; Kirmse, R.; Hoyer, E. *Coord. Chem. Rev.* **1992**, *117*, 99–131.
- (a) Clemenson, P. I. *Coord. Chem. Rev.* **1990**, *106*, 171–203. (b) Davison, A.; Holm, R. H. *Metal Complexes Derived from cis-1,2-Dicyano-1,2-ethylenedithiolate and Bis(trifluoromethyl)-1,2-dithiethane*. *Inorganic Synthesis*; McGraw-Hill, Inc.: New York, 1967; Vol. 10, pp 8–25.
- Manoharan, P. T.; Noordik, J. H.; de Boer, E.; Keijzers, C. P. *J. Chem. Phys.* **1981**, *74*, 1980.
- Kuppusamy, P.; Manoharan, P. T. *Chem. Phys. Lett.* **1985**, *118*, 159–63.
- Veldhuizen, Y. S. J.; Veldman, N.; Spek, A. L.; Faulmann, C.; Haasnoot, J. G.; Reedijk, J. *Inorg. Chem.* **1995**, *34*, 140–7.
- Fourmigue, M.; Lenoir, C.; Coulon, C.; Guyon, F.; Amaudrut, J. *Inorg. Chem.* **1995**, *34*, 4979–85.
- Pilato, R. S.; Gea, Y.; Eriksen, K. A.; Greaney, M. A.; Stiefel, E. I.; Goswami, S.; Kilpatrick, L.; Spiro, T. G.; Taylor, E. C.; Rheingold, A. L. In *Pterins, Quinoxalines, and Metallo-Enedithiolates; Synthetic Approach to the Molybdenum Cofactor*; ACS Symposium Series 535; Stiefel, E. I., Coucouvanis, D., Newton, W. E., Eds.; American Chemical Society: Washington, D.C., **1993**; pp 83–97.
- Armstrong, E. M.; Austerberry, M. S.; Birks, J. H.; Beddoes, R. L.; Helliwell, M.; Joule, J. A.; Garner, C. D. *Heterocycles* **1993**, *35*, 563–8.
- Soricelli, C. L.; Szalai, V. A.; Burgmayer, S. J. *N. J. Am. Chem. Soc.* **1991**, *113*, 9877–8.
- Das, S. K.; Chaudhury, P. K.; Biswas, D.; Sarkar, S. *J. Am. Chem. Soc.* **1994**, *116*, 9061–70.
- Oku, H.; Ueyama, N.; Nakamura, A.; Kai, Y.; Kanehisa, N. *Chem. Lett.* **1994**, 607–10.

application of this method to the synthesis of (dppe)M{S₂C₂-(R)(R')} (M = Ni, Pd, and Pt, and R (R') = 2-, 3-, and 4-pyridine (H), 2-pyrazine (H), and 2-quinoxaline (H or Me)). These complexes were ultimately prepared to determine if the platinum complexes were emissive. These complexes were found to be room temperature solution lumiphores with excited state reactivity that varied with the appended heterocycle.¹⁶ To properly assign the lowest energy electronic transition of the platinum complexes, and thus the emissive states, several of the corresponding nickel and palladium complexes were also prepared.

In addition to serving as a luminescent chromophore, the heterocyclic substituted 1,2-enedithiolate complexes are more

- (a) Cummings, D. S.; Eisenberg, R. *Inorg. Chem.* **1995**, *34*, 2007–14. (b) Bevilacqua, M. J.; Eisenberg, R. *Inorg. Chem.* **1994**, *33*, 2913–23. (c) Cummings, D. S.; Eisenberg, R. *J. Am. Chem. Soc.* **1996**, *118*, 1949–60. (d) Cummings, D. S.; Eisenberg, R. *Inorg. Chem.* **1995**, *34*, 3396–403.
- Zhang, Y.; Ley, K. D.; Schanze, K. S. *Inorg. Chem.* **1996**, *35*, 7102–10.
- (a) Kaiwar, S. P.; Vodacek, A.; Blough, N. V.; Pilato, R. S. *J. Am. Chem. Soc.* **1997**, *119*, 3311–16. (b) Kaiwar, S. P.; Vodacek, A.; Blough, N. V.; Pilato, R. S. *J. Am. Chem. Soc.*, in press. (Protonation State Dependent Excited State Electron Transfer Reactions of Pyridinium Substituted Metallo-1,2-enedithiolates).
- Hsu, J. K.; Bonangelino, C. J.; Kaiwar, S. P.; Boggs, C. M.; Fettingner, J. C.; Pilato, R. S. *Inorg. Chem.* **1996**, *35*, 4743–51.
- Caputo, R.; Ferreri, C.; Palumbo, G. *Synthesis* **1991**, 223–4.
- Caputo, R.; Ferreri, C.; Palumbo, G. *Tetrahedron* **1986**, *42*, 2369–76.
- Wood, W. *Trends in the Chemistry of 1,3-Dithioacetals*; Organosulfur Chemistry, Synthetic Aspects; Page, P., Ed.; Academic Press: San Diego, CA, 1995; pp 133–224.

Scheme 1



basic than the free heterocycle and this increased basicity is metal independent.

Results and Discussion

Reaction of the bis(hydrosulfido) complexes (dppe)M(SH)₂, where; dppe = 1,2-bis(diphenyldiphosphino)ethane and M = Ni, Pd, and Pt²¹ with the α -bromoketones, **4**–**9**^{22–24} yielded the corresponding quinoxalinium-, pyridinium-, and pyrazinium-substituted metallo-1,2-enedithiolate complexes **10**–**23** (Scheme 1). Complexes **24**–**37** were generated upon the addition of triethylamine. Analytically pure samples of **24**–**37** were isolated by subsequent alumina column chromatography. Complexes **10**–**23** could be regenerated quantitatively as the tetrafluoroborate salts by the addition of HBF₄·OEt₂ to solutions of **24**–**37**, respectively.²⁵ Since the (dppe)Ni and Pd analogs of **13/27** and **20/34** were not deemed necessary to assign the electronic transitions of the Pt complexes and since it is unlikely that the Ni and Pd derivatives would be emissive, they were not prepared. These (dppe)Ni and Pd analogs should be available using the procedures outlined for **27** and **34**, respectively.

X-ray Crystallographic Results for 35. The solid state structure of **35** is similar to that of other group VIII metallo-1,2-enedithiolate complexes (Figure 1 and Table 1).^{3b,26} The S(1)–Ni–S(2) angle of 91.89(4)°, the P(1)–Ni–P(2) angle of 86.85(4)°, and the coplanarity of Ni, S(1), S(2), P(1), and P(2),

Table 1. Crystallographic Data for **35**

formula	C ₂₂ H ₂₈ N ₂ NiP ₂ S ₂
formula weight	625.33
space group	Pc2 ₁ /c
a(Å)	12.2522(2)
b(Å)	17.1482(3)
c(Å)	15.0820(3)
β (deg)	92.3750(10)
V(Å ³)	3166.05(10)
Z	4
cryst color, habit	green blade
D _{calc} (g/cm ⁻³)	1.312
μ (Mo K α), cm ⁻¹	8.69
T(K)	218(2)
diffractometer	Siemens P4
radiation	Mo K α (λ = 0.710 73 Å)
R(F) (%) ^a	5.63
R(wF) (%) ^a	11.84

^a Quantity minimized = $R(wF)^2 = \sum[w(F_o^2 - F_c^2)^2] / \sum[w(F_o^2)^2]$; $R = \sum\Delta / \sum(F_o)$, $\Delta = |F_o - F_c|$.

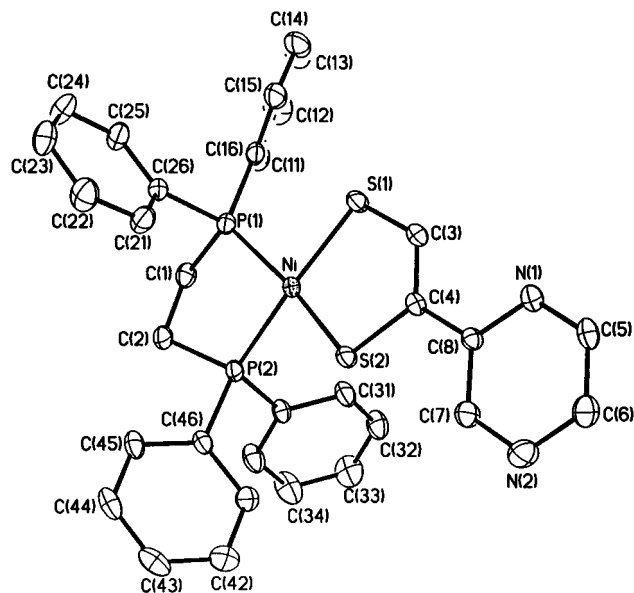


Figure 1. An ORTEP drawing of **35** with the thermal ellipsoids drawn at 50% probability. Selected bond lengths (Å) and angles (deg) are as follows: Ni–S(1), 2.1688(11); Ni–S(2), 2.1626(11); S(1)–C(3), 1.744(4); S(2)–C(4), 1.777(4); C(3)–C(4), 1.346(5); C(4)–C(8), 1.472(5); S(1)–Ni–S(2), 91.89(4); Ni–S(1)–C(3), 103.57(13); Ni–S(2)–C(4), 104.24(13); S(1)–C(3)–C(4), 121.9(3); S(2)–C(4)–C(3), 118.3(3).

with no atom deviating from the least squares plane by more than 0.16 Å, are all expected for a bis(phosphine)-ligated Ni(II) complex. The Ni–S and C–S bonds of **35** are best

- (21) (a) Schmidt, M.; Hoffmann, G. G.; Holler, R. *Inorg. Chim. Acta* **1979**, *32*, L19–L20. (b) The reported ¹H NMR resonances for the hydrosulfido ligands of **1**–**3** were improperly assigned; the proper assignments are listed. **1** (dppe)Ni(SH)₂: ¹H NMR (CDCl₃) δ –0.77 (second-order multiplet, 2H, SH, major line spacing = 15 Hz). **2** (dppe)Pd(SH)₂: ¹H NMR (CDCl₃) δ –0.55 (second-order multiplet, 2H, SH, line spacings = 11 and 6 Hz). **3** (dppe)Pt(SH)₂: ¹H NMR (CDCl₃); δ –0.29 (second-order multiplet with platinum satellites, 2H, SH, line spacings = 11 and 6 Hz with a J_{Pt-H} = 53 Hz). There was no field or temperature dependence of the second-order line spacings.
- (22) Rowe, D. J.; Garner, C. D.; Joule, J. A. *J. Chem. Soc., Perkin Trans. 1* **1985**, 1907–10.
- (23) Menasse, R. v.; Klein, G.; Erlenmeyer, H. *Helv. Chim. Acta* **1955**, *38*, 1289–91.
- (24) Easmon, J.; Heinisch, G.; Holzer, W.; Rosenwirth, B. *J. Med. Chem.* **1992**, *35*, 3288–96.
- (25) While complexes **24**–**37** were isolated analytically pure, no attempts to prepare **10**–**23** analytically pure were made. However, the protonation/deprotonation was repeated 10 times with no loss in absorption of either the protonated or deprotonated complexes.
- (26) (a) Sartain, D.; Truter, M. R. *J. Chem. Soc. A* **1965**, 1264–72. (b) Kato, R.; Kobayashi, H.; Kobayashi, A.; Sasalo, Y. *Chem. Lett.* **1985**, 131–4. (c) Bevilacqua, M. J.; Zuleta, A. J.; Eisenberg, R. *Inorg. Chem.* **1993**, *32*, 3689–93. (d) Baird, H. W.; Whilet B. M. *J. Am. Chem. Soc.* **1966**, *88*, 4744. (e) Churchill, M. R.; Gennessy, J. P. *Inorg. Chem.* **1968**, *7*, 1123. (f) Miller, E. J.; Brill, T. B.; Rheingold, A. L.; Fultz, W. C. *J. Am. Chem. Soc.* **1983**, *105*, 7580.

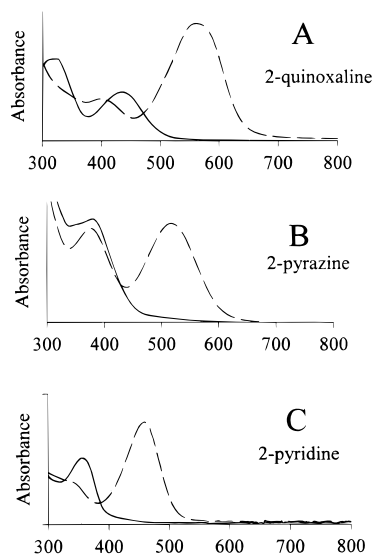


Figure 2. UV-vis absorption spectra in CH_3CN of the corresponding 2-quinoxaline(ium)-, 2-pyridine(ium)-, and 2-pyrazine(ium)-substituted 1,2-enedithiolates of $(\text{dppe})\text{Pt}$: (A) **26** (solid) and **12** (dashed); (B) **30** (solid) and **16** (dashed); (C) **37** (solid) and **23** (dashed).

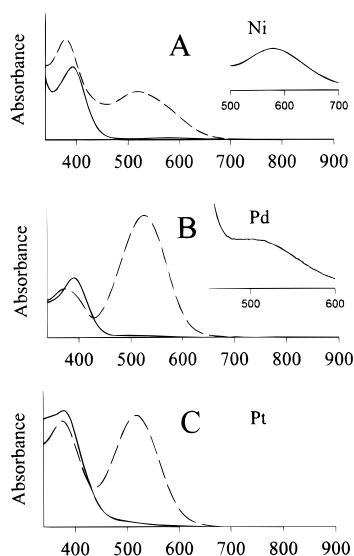


Figure 3. UV-vis absorption spectra in CH_3CN of the corresponding $(\text{dppe})\text{M}\{\text{S}_2\text{C}_2(2\text{-pyrazine})(\text{H})\}$ and $(\text{dppe})\text{M}\{\text{S}_2\text{C}_2(2\text{-pyrazinium})(\text{H})\}$ $\text{M} = \text{Ni}, \text{Pd},$ and Pt complexes: (A) **35** (solid) and **21** (dashed); (B) **36** (solid) and **22** (dashed); (C) **37** (solid) and **23** (dashed). The insets ($\times 40$) show low-lying d to d transitions for **35** and **36**; the corresponding band in the platinum complex, **37**, is obscured by the ILCT transition. From the study of **30**, **33**, and **34** this band is thought to be at ≈ 410 nm.

described as single bonds while $\text{C}(3)\text{--}\text{C}(4)$, at $1.346(5)$ Å, is best described as a double bond. The metallo-1,2-enedithiolate is a planar five-membered ring (with no atom deviating from the least squares plane by more than 0.02 Å), and the pyrazine is a planar six-membered ring (with no atom deviating from the least squares plane by more than 0.022 Å). The pyrazine is $\approx 6^\circ$ from being coplanar with the metallo-1,2-enedithiolate.

Electronic Spectra. All of the complexes prepared in this study have a UV-visible band assignable to a 1,2-enedithiolate $\pi \rightarrow$ heterocyclic π^* charge transfer (ILCT) transition (Figures 2 and 3, Table 2). The energy of this band is sensitive to solvent polarity, decreasing by 1000 cm^{-1} from CCl_4 to DMSO for the neutral complexes and increasing by 1000 cm^{-1} for the protonated complexes. While this supports the charge transfer assignment, the energies of these bands are nearly identical for the corresponding Ni, Pd, and Pt 1,2-enedithiolate complexes (Table 2, Figure 3), ruling out assignment to a MLCT, LMCT,

or d to d transition.²⁷ Replacing H (**26/12**) with Me (**27/13**) and protonation of the heterocycles both red-shift this transition (Table 2). Since methyl substitution makes the 1,2-enedithiolate a better donor, while protonation makes the heterocycle a better acceptor, the observed red shifts are consistent with an intraligand transition.

Further evidence supporting the ILCT assignment came from a plot of heterocycle reduction potential vs the absorption energy of the ILCT band for the corresponding $(\text{dppe})\text{M}\{\text{S}_2\text{C}_2(\text{heterocycle})(\text{H})\}$ complex (Figure 4). This plot shows the linear relationship between the energy of the ILCT transition and the electron affinity of the aromatic heterocycle.²⁸ Since the π^* orbital is the electron acceptor in the reduction, it is inferred from this plot that the heterocycle π^* orbital is the acceptor in the electronic transition.

This crude plot also makes it possible to predict the ILCT transition energy of a yet unknown $(\text{dppe})\text{M}\{\text{S}_2\text{C}_2(\text{heterocycle})(\text{H})\}$ complex by knowing only the reduction potential of the appended heterocycle.²⁸ It is generally either a weak metal dependent band or the ILCT band that is the lowest energy electronic transition in these complexes. Since the energy of the metal dependent transition does not appear to change substantially with changes in the 1,2-enedithiolate appended heterocycle (Table 2, Figure 4), using this plot it should be possible to predict when the ILCT transition will be the lowest energy band prior to the synthesis of a new metal complex.²⁹ It should also be possible to predict when protonation of the heterocycle is required to make the ILCT transition the lowest energy band. We have demonstrated that $(\text{dppe})\text{Pt}$ complexes with low-lying ILCT transitions are emissive in room temperature solution.¹⁶ Being able to control the energy of this transition by heterocycle selection (based on reduction potential) or heterocycle protonation is particularly useful in the design of new emissive complexes with unique excited state properties.

Resonance Stabilization of the Protonated Heterocycle and $\text{p}K_a$. Resonance stabilization of a protonated heterocycle by a metallo-1,2-enedithiolate was shown in a previous study to increase the basicity of the appended heterocycle.¹⁷ Consistent with these findings, in acetonitrile the $\text{p}K_a$ values of the 2- and 4-pyridinium-substituted complexes **16** and **20** are ≈ 3 units higher than that of pyridinium (Table 3).³⁰ The relatively low $\text{p}K_a$ of **19** is attributed to the lack of resonance stabilization of the protonated 3-heterocycle.¹⁷

The $\text{p}K_a$ value for quinoxalinium is not known in acetonitrile, but from the aqueous value and the water-to-acetonitrile $\text{p}K_a$ shifts of other aromatic heterocycles it is assumed to be in the 9–10 range.^{31,32} As such, the quinoxaline-substituted complexes, like their 2- and 4-pyridine analogs, are more basic than the free heterocycle by 2–3 $\text{p}K_a$ units.

- (27) (a) Shupack, S. I.; Billig, E. C.; Williams, R.; Gray, H. B. *J. Am. Chem. Soc.* **1964**, *86*, 4594–602. (b) Gray, H. B.; Ballhausen, C. J. *J. Am. Chem. Soc.* **1963**, *85*, 260–4.
- (28) (a) Jordan, K. D.; Burrow, P. D. *Acc. Chem. Res.* **1978**, *11*, 341–8. (b) Wiberg, K. B.; Lewis, T. P. *J. Am. Chem. Soc.* **1970**, *92*, 7154–60.
- (29) Given the reduction potentials for nitrobenzene (-0.98 V) and 2-bromopyridine (-2.0 V) the ILCT transition energies for $(\text{dppe})\text{Pt}\{\text{S}_2\text{C}_2(\text{pyridin-2-yl 5-bromide})(\text{H})\}$ ($21\,320\text{ cm}^{-1}$) and $(\text{dppe})\text{Pt}\{\text{S}_2\text{C}_2(4\text{-nitrobenzene})(\text{H})\}$ ($26\,880\text{ cm}^{-1}$) correlate with the plot shown in Figure 4 unpublished results.
- (30) (a) Coetzee, J. F.; Padmanabhan, G. R. *J. Am. Chem. Soc.* **1965**, *87*, 5005–10. (b) Coetzee, J. F. *Ionic Reactions in Acetonitrile*; Progress in Physical Organic Chemistry; Streitwieser, A. J. Taft, R. W., Eds.; Interscience Publishers: New York, **1967**, 45–92.
- (31) (a) Perrin, D. D. *Dissociation Constants of Organic Bases in Aqueous Solution*; Butterworth & Co.: London, 1972; Vol. 1. (b) Perrin, D. D. *Dissociation Constants of Organic Bases in Aqueous Solution*; Butterworth & Co.: London, 1965; Vol. 2.
- (32) Moore, E. J.; Sullivan, J. M.; Norton, J. R. *J. Am. Chem. Soc.* **1986**, *108*, 2257–63.

Table 2. UV-Visible Bands for Complexes **10–37** (CH₂Cl₂)

complex	M	R, R'	λ_{\max} (ϵ)	
			neutral ^a	protonated ^a
24, 10	Ni	quin, H	346 (6000), <u>444</u> (5700), 580 (90)	372 (4,300), <u>568</u> (11000)
25, 11	Pd	quin, H	342 (5200), <u>443</u> (5300), 520 (80)	392 (4,900), <u>564</u> (11700)
26, 12	Pt	quin, H	326 (9400), <u>442</u> (6000)	396 (5,600), <u>564</u> (11600)
27, 13	Pt	quin, Me	328 (13300), <u>464</u> (5,300)	313 (12900), <u>428</u> (9800), <u>605</u> (15900)
28, 14	Ni	2-py, H	<u>367</u> (4500), 584 (90)	376 (2700), <u>462</u> (7000)
29, 15	Pd	2-py, H	<u>360</u> (4000), 519 (90)	343 (sh, 3200), <u>456</u> (5700)
30, 16	Pt	2-py, H	<u>358</u> (4300), 415 (sh, 380)	336 (sh, 2800), <u>458</u> (6600)
31, 17	Ni	3-py, H	<u>358</u> (4900), 586 (90)	378 (5800), <u>444</u> (sh, 2100)
32, 18	Pd	3-py, H	<u>352</u> (4400), 520 (80)	<u>382</u> (4600), <u>446</u> (sh, 1600)
33, 19	Pt	3-py, H	<u>346</u> (6000), 410 (sh, 450)	<u>374</u> (6200), <u>460</u> (sh, 2100)
34, 20	Pt	4-py, H	<u>360</u> (3900), 410 (sh, 560)	<u>342</u> (3800), <u>474</u> (5900)
35, 21	Ni	2-pyra, H	<u>393</u> (7700), 590 (205)	380 (10500), <u>521</u> (5100)
36, 22	Pd	2-pyra, H	<u>390</u> (7470), 520 (80)	345 (12100), <u>530</u> (5400)
37, 23	Pt	2-pyra, H	<u>360</u> (5100), <u>382</u> (6800)	380 (11600), <u>521</u> (15,000)

^a λ_{\max} in nm. The bands assigned to the ILCT transitions are underlined.

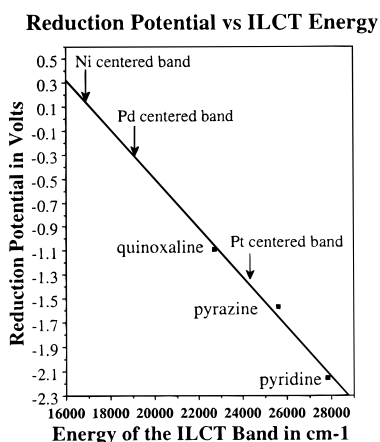


Figure 4. A plot of heterocycle reduction potential versus the energy of the ILCT band (CH₃CN) for the corresponding (dppe)M{S₂C₂(2-heterocycle)(H)} complexes where M = Ni, Pd, or Pt. Also shown is the approximate energy of the lowest lying metal dependent transition in the Ni, Pd, and Pt complexes. The ILCT transition is independent of metal while the metal dependent transition (presumably d → d) is independent of heterocycle.

Table 3. pK_a Values for Complexes **10–12, 16, 19, and 20** in Acetonitrile

complex	M	R, R'	pK
10	Ni	2-quinoxalinium, H	11.7 ± 0.2
11	Pd	2-quinoxalinium, H	11.9 ± 0.2
12	Pt	2-quinoxalinium, H	11.9 ± 0.2
16	Pt	2-pyridinium, H	15.4 ± 0.2
19	Pt	3-pyridinium, H	13.8 ± 0.2
20	Pt	4-pyridinium, H	15.6 ± 0.1
		free quinoxalinium	≈9 ^a
		free pyridinium	12.3 ± 0.1

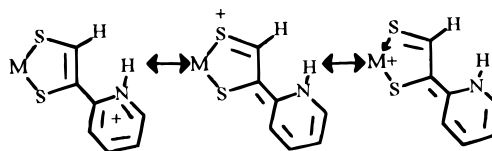
^a Estimated from the aqueous value assuming the ≈8 pK_a shift observed for other protonated aromatic heterocycles.

The pK_a values obtained for **10–12, 16, 19, and 20** were nearly identical to those of the corresponding Cp₂Mo{S₂C₂-(heterocycle)(R)} complexes.¹⁷ The lack of a metal dependence upon the pK_a of these complexes suggests that a resonance form that localizes the positive charge on a sulfur atom of the 1,2-enedithiolate ligand, rather than the metal, is most important to the increased basicity (Scheme 2). On the basis of the pK_a of 2-, 3-, and 4-aminopyridinium,³¹ the 1,2-enedithiolate appears to be as effective at resonance stabilizing pyridinium as an amino functional group.

Conclusion

Modeled after the synthesis of 1,4-dithiins, a new method to produce metallo-1,2-enedithiolates was applied to the synthesis

Scheme 2



of a range of (dppe)M{S₂C₂(R)(R')} derivatives. Unlike 1,4-dithiin synthesis, this new route to metallo-1,2-enedithiolates did not require dehydrating conditions and was tolerant of several heterocyclic functional groups.^{18–20}

This study has also served to demonstrate that the 1,2-enedithiolate ligand can increase the basicity of an appended heterocycle. This effect was most prevalent in the 2- and 4-substituted heterocycles where resonance stabilization of the protonated heterocycle by the 1,2-enedithiolate ligand was possible. The nearly equivalent pK_a of the corresponding (dppe)M (M= Ni, Pd, and Pt) and Cp₂Mo complexes¹⁷ suggests that the increased basicity is due to a dominant resonance form that localizes positive charge upon a sulfur atom and not the metal center of these complexes.

The complexes described in this paper were ultimately prepared in an attempt to design new emissive platinum complexes and to allow assignment of the excited states. The versatility of this method has allowed several heterocycles to be appended to the 1,2-enedithiolate ligand, including 2-, 3-, and 4-pyridine, 2-pyrazine, and 2-quinoxaline along with their protonated analogs. Of these complexes, the platinum 2- and 4-pyridinium-, 2-pyrazinium- and 2-quinoxaline-substituted 1,2-enedithiolate complexes were emissive with ILCT* excited states.¹⁶ Since the reduction potential of the appended heterocycle controls the energy of the ILCT transition and determines whether it will be the lowest energy band, the emissions from these complexes should be easily tuned by heterocycle selection and by heterocycle protonation.

Experimental

Materials. (dppe)M(SH)₂ (where M = Ni, Pd, and Pt and dppe = 1,2-bis(diphenylphosphino)ethane),²¹ 1-quinoxalin-2-yl-2-bromoethanone,²² 1-quinoxalin-2-yl-2-bromopropanone,²² 1-pyridin-2-yl-, 1-pyridin-3-yl-, and 1-pyridin-4-yl-2-bromoethanone,²³ and 1-pyrazin-2-yl-2-bromoethanone²⁴ were prepared according to the literature procedures. All reactions were performed under an atmosphere of nitrogen using standard Schlenk line techniques. Workups were performed in air unless stated otherwise. Dichloromethane, acetonitrile, and pentane were dried over calcium hydride and distilled under nitrogen. Diethyl ether, tetrahydrofuran, and dioxane were dried over Na/benzophenone and distilled under nitrogen. Triethylamine was dried over potassium hydroxide and vacuum distilled. DMF was used as received from Aldrich Chemical. Neutral activated alumina, 80–325 mesh, was

purchased from EM Science, Cherry Hill, NJ, and treated with 6% H₂O by weight to generate the Brockmann activity 3 material used throughout this study.

Physical Measurements. NMR spectra were acquired with a Bruker AF 200 or a Bruker AM 400. IR spectra were collected either with a Perkin Elmer 1600 or a Nicolet 5 DXL FT-IR spectrometer. UV-visible spectra were recorded on either a Perkin Elmer Lambda 2S or a Hewlett Packard 8452A spectrometer. EI and FAB mass spectral data were collected on a Magnetic Sector VG 7070E. Chemical analyses were performed by M-H-W Laboratories, Phoenix, AZ.

Synthesis. (dppe)Ni{S₂C₂(2-quinoxaline)(H)}·CH₂Cl₂ (24). To a DMF (5 mL) solution of (dppe)Ni(SH)₂ (314 mg, 0.60 mmol) was added 1-quinoxalin-2-yl-2-bromoethanone (150 mg, 0.62 mmol). The solution became purple over a period of 20 min. The DMF was removed from the resulting purple solution, and the solid was washed with 3 × 20 mL of diethyl ether. The purple solid was dissolved in dichloromethane (5 mL), and triethylamine was added dropwise to the solution until it was orange red. The solvent was removed in air, and the solid was chromatographed on a 1 × 20 cm alumina column, where the product eluted with 1:2 hexane-CH₂Cl₂. The eluent was evaporated to dryness to give **24** as an orange-red crystalline solid in 43% yield (190 mg, 0.26 mmol). Anal. Calcd for C₃₇Cl₂H₃₂N₂P₂S₂Ni: C, 58.42; H, 4.21; N, 3.68. Found: C, 58.82; H, 4.49; N, 3.49. ¹H NMR (CDCl₃): δ 9.27 (s, 1H, C₈H₅N₂), 7.94 (d, 1H, S₂C₂H, J_{P-H} = 8 Hz), 7.90 (d, 1H, C₈H₅N₂, J_{H-H} = 8 Hz), 7.88 (d, 1H, C₈H₅N₂, J_{H-H} = 8 Hz), 7.82–7.77 (m, 8H, PC₆H₅), 7.61–7.54 (m, 2H, C₆H₄N₂), 7.51–7.44 (m, 12H, PC₆H₅), 2.39 (d, 4H, PC₂H₂, J_{P-H} = 18 Hz). ³¹P NMR (CDCl₃): δ 58.5 (broad s), 58.2 (broad s). Mass spectrum (FAB) *m/z* = 675 (M⁺), 456 (M⁺ - C₁₀H₆N₂S₂). UV-vis (abs) λ_{max} (ε) (CH₂Cl₂, nm): 240 (24 927), 276 (20 223) 302 (16 000), 346 (sh) (6000), 444 (5700), 580 (90). IR (KBr, cm⁻¹): 3052 (w), 2946 (w), 2903 (w), 1540 (m), 1506 (vs), 1475 (m), 1435 (vs), 1406 (w), 1330 (w), 1301 (w), 1284 (w), 1265 (w), 1207 (m), 1187 (w), 1129 (w), 1099 (s), 1027 (w), 999 (m), 922 (w), 876 (m) 830 (w), 818 (m), 761 (w), 746 (m), 713 (s), 690 (vs), 530 (vs), 484 (m).

(dppe)Pd{S₂C₂(2-quinoxaline)(H)} (25) was prepared and isolated as described for complex **24**, using (dppe)Pd(SH)₂ (342 mg, 0.60 mmol) and 1-quinoxalin-2-yl-2-bromoethanone (150 mg, 0.62 mmol). Complex **25** was isolated in 53% yield (230 mg, 0.32 mmol). Anal. Calcd for C₃₆H₃₀N₂P₂PdS₂: C, 59.83; H, 4.16; N, 3.88. Found: C, 59.72; H, 4.37; N, 3.89. ¹H NMR (CDCl₃): δ 9.32 (s, 1H, C₈H₅N₂), 7.99 (d, 1H, S₂C₂H, J_{P-H} = 8 Hz), 7.97 (d, 1H, C₈H₅N₂, J_{H-H} = 8 Hz), 7.85 (d, 1H, C₈H₅N₂, J_{H-H} = 8 Hz), 7.83–7.76 (m, 8H, PC₆H₅), 7.50–7.47 (m, 2H, C₆H₅ N₂), 7.47–7.42 (m, 12H, PC₆H₅), 2.51 (d, 4H, PC₂H₂, J_{P-H} = 21 Hz). ³¹P NMR (CDCl₃): δ 51.4 (d, J_{P-P} = 15 Hz), 51.2 (d, J_{P-P} = 15 Hz). Mass spectrum (FAB) *m/z* = 723 (M⁺), 506 (M⁺ - C₁₀H₆N₂S₂). UV-vis (abs) λ_{max} (ε) (CH₂Cl₂, nm): 240 (21 000), 281 (15 500), 308 (11 500), 342 (5200), 443 (5300), 520 (80). IR (KBr, cm⁻¹): 3048 (w), 2947 (w), 2903 (w), 1540 (m), 1504 (vs), 1477 (m), 1435 (vs), 1412 (w), 1330 (w), 1306 (w), 1284 (w), 1265 (w), 1207 (m), 1187 (w), 1130 (w), 1102 (s), 1027 (w), 999 (m), 920 (w), 877 (m) 855 (w), 821 (m), 799 (w), 761 (w), 748 (m), 714 (s), 690 (vs), 530 (vs), 484 (m).

(dppe)Pt{S₂C₂(2-quinoxaline)(H)}·CH₂Cl₂ (26) was prepared and isolated as described for complex **24**, using (dppe)Pt(SH)₂ (132 mg, 0.20 mmol) and 1-quinoxalin-2-yl-2-bromoethanone (53 mg, 0.21 mmol). Complex **26** was isolated in 40% yield (70 mg, 0.080 mmol). Anal. Calcd for C₃₇H₃₂Cl₂N₂PtS₂: C, 49.55; H, 3.57; N, 3.13. Found: C, 49.88; H, 3.31; N, 3.07. ¹H NMR (CDCl₃): δ 9.33 (s, 1H, C₈H₅N₂), 8.35 (d with Pt satellites, 1H, S₂C₂H, J_{P-H} = 7 Hz; J_{Pt-H} = 95 Hz), 7.97 (d, 1H, C₈H₅N₂, J_{H-H} = 7 Hz), 7.89 (d, 1H, C₈H₅N₂, J_{H-H} = 7 Hz), 7.83–7.77 (m, 8H, PC₆H₅), 7.58–7.51 (m, 2H, C₆H₅N₂), 7.50–7.44 (m, 12H, PC₆H₅), 2.51 (d, 4H, PC₂H₂, J_{P-H} = 18 Hz; J_{Pt-H} = 55 Hz). ³¹P NMR (CDCl₃): δ 45.7 (d with Pt satellites, J_{P-P} = 14 Hz; J_{Pt-P} = 2780 Hz), 45.0 (d with Pt satellites, J_{P-P} = 14 Hz; J_{Pt-P} = 2728 Hz). Mass spectrum (FAB) *m/z* = 812 (M⁺), 594 (M⁺ - C₁₀H₆N₂S₂). UV-vis (abs) λ_{max} (ε) (CH₂Cl₂, nm): 244 (29 900), 274 (26 800), 306 (8400), 326 (9400), 442 (6000). IR (KBr, cm⁻¹): 3048 (w), 2947 (w), 2915 (w), 2849 (w), 1540 (m), 1506 (vs), 1483 (m), 1435 (vs), 1412 (w), 1330 (w), 1301 (w), 1280 (w), 1265 (w), 1207 (m), 1187 (w), 1131 (w), 1103 (s), 1027 (w), 999 (m), 920 (w), 879 (m) 855 (w), 820 (m), 799 (w), 750 (m), 748 (m), 714 (s), 690 (vs), 531 (vs), 484 (m).

(dppe)Pt{S₂C₂(2-quinoxaline)(Me)} (27) was prepared and isolated as described for complex **24**, using (dppe)Pt(SH)₂ (132 mg, 0.20 mmol) and 1-quinoxalin-2-yl-2-bromopropanone (56 mg, 0.22 mmol). Complex **27** was obtained as an orange red crystalline solid in 49% yield (81 mg, 0.098 mmol). Anal. Calcd for C₃₇H₃₂N₂P₂PtS₂: C, 53.82; H, 3.88; N, 3.39. Found: C, 54.12; H, 4.09; N, 3.15. ¹H NMR (CDCl₃): δ 9.14 (s, 1H, C₈H₅N₂), 7.98 (d, 1H, C₈H₅N₂, J_{H-H} = 7 Hz), 7.95 (d, 1H, C₈H₅N₂, J_{H-H} = 7 Hz), 7.88–7.76 (m, 8H, PC₆H₅), 7.71–7.63 (m, 2H, C₆H₅N₂), 7.53–7.48 (m, 12H, PC₆H₅), 2.53 (d, 4H, PCH₂, J_{P-H} = 18 Hz; J_{Pt-H} = 54 Hz), 2.39 (s, 3H, CH₃). ³¹P NMR (CDCl₃): δ 45.1 (d with Pt satellites, J_{P-P} = 15 Hz; J_{Pt-P} = 2780 Hz), 44.7 (d with Pt satellites, J_{P-P} = 15 Hz; J_{Pt-P} = 2756 Hz). Mass spectrum (FAB) *m/z* = 826 (M⁺), 627 (M⁺ - C₁₁H₈N₂S). UV-vis (abs) λ_{max} (ε) (CH₂Cl₂, nm): 248 (23 500), 270 (25 100), 310 (14 600), 328 (13 300) 461 (4300). IR (KBr, cm⁻¹): 3038 (w), 2923 (w), 2846 (w), 1511 (s), 1489 (m), 1436 (vs), 1412 (w), 1339 (w), 1301 (w), 1268 (w), 1202 (m), 1136 (w), 1103 (s), 1027 (w), 998 (m), 938 (w), 880 (m) 824 (m), 750 (m), 748 (m), 714 (s), 691 (vs), 531 (vs), 484 (m).

(dppe)Ni{S₂C₂(2-pyridine)(H)} (28) was prepared and isolated as described for complex **24**, using 1-pyridin-2-yl-2-bromoethanone (0.025 g, 0.125 mmol) and (dppe)Ni(SH)₂ (0.052 g, 0.1 mmol). Complex **28** was isolated as a green solid in 29% yield (0.018 g, 0.029 mmol). Anal. Calcd for C₃₃H₂₉NNiP₂S₂: C, 63.46; H, 4.65; N, 2.24. Found: C, 63.33; H, 4.52; N, 1.93. ¹H NMR (CDCl₃): δ 8.36 (d, 1H, C₅H₄ N, J_{H-H} = 4 Hz), 7.99 (d, 1H, S₂C₂H, J_{P-H} = 6 Hz), 7.80–7.71 (m, 8H, PC₆H₅), 7.66 (d, 1H, C₅H₄ N, J_{H-H} = 6 Hz), 7.50 (m, 1H, C₅H₄ N), 7.46–7.40 (m, 12H, PC₆H₅), 6.85 (m, 1H, C₅H₄ N), 2.37 (m, 2H, PC₂H₂), 2.33 (m, 2H, PC₂H₂). ³¹P NMR (CDCl₃): δ 57.4 (broad singlet), 57.2 (broad singlet). Mass spectrum (FAB) *m/z* = 624 (M⁺), 489 (M⁺ - C₇H₅NS₂). UV-vis (abs) λ_{max} (ε) (CH₂Cl₂, nm): 367 (4540), 584 (90). IR (KBr, cm⁻¹): 3050 (w), 2962 (w), 2908 (w), 1578 (m), 1508 (m), 1482 (m), 1459 (vs), 1436 (vs), 1420 (m), 1313 (w), 1262 (m), 1189 (vs), 1174 (s), 1119(s), 1102 (vs), 1070 (m), 1026 (m), 998 (m), 932 (w), 881 (w), 796 (m), 735 (vs), 715 (s), 692 (vs), 622 (s), 611 (s), 543 (m), 532 (m), 514 (s), 501(s), 484 (m).

(dppe)Pd{S₂C₂(2-pyridine)(H)} (29) was prepared and isolated as described for complex **24**, using (dppe)Pd(SH)₂ (0.057 g, 0.1 mmol) and 1-pyridin-2-yl-2-bromoethanone (0.025 g, 0.125 mmol). Complex **29** was isolated as a pink crystalline solid in 31% yield (21 mg, 0.03 mmol). Anal. Calcd for C₃₃H₂₉NP₂PdS₂: C, 58.98; H, 4.32; N, 2.09. Found: C, 58.69; H, 4.61; N, 1.92. ¹H NMR (CDCl₃): δ 8.38 (m, 1H, C₅H₄ N), 8.00 (dd, 1H, S₂C₂H, J_{P-H} = 6 Hz; J_{P-H} = 1 Hz), 7.86–7.76 (m, 8H, PC₆H₅), 7.73 (d, 1H, C₅H₄ N, J_{H-H} = 8 Hz), 7.60 (m, 1H, C₅H₄ N), 7.54–7.49 (m, 12H, PC₆H₅), 6.99 (m, 1H, C₅H₄ N), 2.59 (m, 2H, PC₂H₂), 2.53 (m, 2H, PC₂H₂). ³¹P NMR (CDCl₃): δ 50.7 (d, J_{P-P} = 15 Hz), 50.2 (d, J_{P-P} = 15 Hz). Mass spectrum (FAB) *m/z* = 672 (M⁺), 504 (M⁺ - C₇H₅NS₂). UV-vis (abs) λ_{max} (ε) (CH₂Cl₂, nm): 298 (5800), 360 (4000), 519 (90). IR (KBr, cm⁻¹): 3046 (w), 2966 (w), 2912 (w), 2877(w), 1578 (m), 1523 (m), 1482 (m), 1459 (m), 1435 (vs), 1406 (w), 1330 (w), 1301 (w), 1284 (w), 1265 (w), 1207 (w), 1186 (w), 1159 (w), 1102 (s), 1026 (w), 997 (m), 930 (w), 877 (m), 820 (m), 761 (w), 746 (m), 715 (s), 704 (s), 690 (vs), 530 (vs), 484 (m).

(dppe)Pt{S₂C₂(2-pyridine)(H)} (30) was prepared and isolated as described for complex **24**, using (dppe)Pt(SH)₂ (0.165 g, 0.25 mmol) and 1-pyridin-2-yl-2-bromoethanone (0.062 g, 0.313 mmol). Complex **30** was isolated as a yellow crystalline solid in 41% yield (78 mg, 0.10 mmol). Anal. Calcd for C₃₃H₂₉NP₂PtS₂: C, 52.04; H, 3.81; N, 1.84. Found: C, 51.88; H, 4.09; N, 1.57. ¹H NMR (CDCl₃): δ 8.38 (m, 1H, C₅H₄ N), 7.96 (dd with ¹⁹⁵Pt satellites, 1H, S₂C₂H, J_{P-H} = 7 Hz; J_{P-H} = 1 Hz; J_{Pt-H} = 95 Hz), 7.88–7.79 (m, 8H, PC₆H₅), 7.69 (d, 1H, C₅H₄ N, J_{H-H} = 8 Hz), 7.57 (m, 1H, C₅H₄ N), 7.52–7.46 (m, 12H, PC₆H₅), 6.94 (m, 1H, C₅H₄ N), 2.55 (m, 2H, PC₂H₂), 2.51 (m, 2H, PC₂H₂). ³¹P NMR (CDCl₃): δ 45.5 (d with Pt satellites, J_{P-P} = 15 Hz; J_{Pt-P} = 2770 Hz), 44.9 (d with Pt satellites, J_{P-P} = 15 Hz; J_{Pt-P} = 2730 Hz). Mass spectrum (FAB) *m/z* = 761 (M⁺), 593 (M⁺ - C₇H₅NS₂). UV-vis (abs) λ_{max} (ε) (CH₂Cl₂, nm): 358 (4300), 415 (sh, 380). IR (KBr, cm⁻¹): 3050 (w), 2963 (w), 2911 (w), 1578 (m), 1522 (m), 1508 (m), 1482 (m), 1459 (m), 1435 (vs), 1310 (w), 1284 (w), 1265 (w), 1207 (m), 1187 (m), 1104 (vs), 1050 (w), 1028 (w), 998 (m), 932 (w), 880 (m), 822 (m), 760 (w), 750 (m), 716 (s), 705(s), 690 (vs), 533 (vs), 486 (m).

(dppe)Ni{S₂C₂(3-pyridine)(H)} (31) was prepared and isolated as described for **24** using 1-pyridin-3-yl-2-bromoethanone (0.025 g, 0.125 mmol) and (dppe)Ni(SH)₂ (0.052 g, 0.1 mmol). Complex **31** was isolated as a green solid in 30% yield (0.019 g, 0.030 mmol). Anal. Calcd for C₃₃H₂₉NNiP₂S₂: C, 63.46; H, 4.65; N, 2.24. Found: C, 63.21; H, 4.78; N, 2.11. ¹H NMR (CDCl₃): δ 8.76 (s, 1H, C₅H₄ N), 8.24 (d, 1H, C₅H₄ N, J_{H-H} = 6 Hz) 7.90 (dd, 1H, S₂C₂H, J_{P-H} = 7 Hz; J_{P-H} = 1 Hz), 7.83–7.56 (m, 8H, PC₆H₅), 7.69 (d, 1H, C₅H₄ N, J_{H-H} = 9 Hz), 7.54–7.47 (m, 12H, PC₆H₅), 7.08 (dd, 1H, C₅H₄ N, J_{H-H} = 9 Hz, J_{H-H} = 6 Hz), 2.46 (m, 2H, PC₂H₂), 2.41 (m, 2H, PC₂H₂). ³¹P NMR (CDCl₃): δ 57.8 (two overlapping broad resonances). Mass spectrum (FAB) *m/z* = 624 (M⁺), 522 (M⁺ – C₇H₅NS). UV–vis (abs) λ_{max} (ε) (CH₂Cl₂): 312 (6000), 358 (4900), 586 (90). IR (KBr): 3050 (w), 2962 (w), 2908 (w), 1588 (m), 1482 (m), 1436 (vs), 1418 (m), 1313 (w), 1262 (s), 1189 (vs), 1174 (s), 1119(s), 1102 (vs), 1070 (m), 1026 (m), 998 (m), 926 (w), 881 (w), 797 (m), 735 (vs), 716 (s), 692 (vs), 622 (s), 611 (s), 543 (m), 532 (m), 514 (s), 501(s), 484 (m).

(dppe)Pd{S₂C₂(3-pyridine)(H)} (32) was prepared and isolated as described for **24** using 1-pyridin-3-yl-2-bromoethanone (0.025 g, 0.125 mmol) and (dppe)Pd(SH)₂ (0.057 g, 0.1 mmol). Complex **32** was isolated as a pink solid in 33% yield (0.022 g, 0.033 mmol). Anal. Calcd for C₃₃H₂₉NP₂PdS₂: C, 58.98; H, 4.32; N, 2.09. Found: C, 58.82; H, 4.66; N, 2.01. ¹H NMR (CDCl₃): δ 8.80 (s, 1H, C₅H₄ N), 8.26 (d, 1H, C₅H₄ N, J_{H-H} = 8 Hz) 7.90 (dd, 1H, S₂C₂H, J_{P-H} = 7 Hz; J_{P-H} = 1 Hz), 7.85–7.76 (m, 8H, PC₆H₅), 7.53–7.49 (m, 12H, PC₆H₅), 7.10 (dd, 1H, C₅H₄ N, J_{H-H} = 8 Hz; J_{H-H} = 5 Hz), 6.97 (d, 1H, C₅H₄ N, J_{H-H} = 5 Hz), 2.59 (m, 2H, PC₂H₂), 2.54 (m, 2H, PC₂H₂). ³¹P NMR (CDCl₃): δ 51.3 (d, J_{P-P} = 10 Hz), 51.0 (d, J_{P-P} = 10 Hz). Mass spectrum (FAB) *m/z* = 672 (M⁺), 504 (M⁺ – C₇H₅NS₂). UV–vis (abs) λ_{max} (ε) (CH₂Cl₂, nm): 298 (6300), 352 (4400), 520 (80). IR (KBr, cm⁻¹): 3049 (w), 3033 (w), 2997 (w), 2926 (w), 1578 (m), 1560 (m), 1534 (s), 1481 (m), 1433 (vs), 1413 (w), 1400 (w), 1328 (w), 1308 (w), 1267 (w), 1236 (w), 1216 (m), 1185 (m), 1158 (w), 1102 (s), 1071 (w), 1041 (w), 1026 (m), 998 (m), 910 (m), 878 (m), 820 (m), 803 (m), 775 (m), 748 (m), 711 (s), 704 (s), 690 (vs), 654 (m), 608 (w), 524 (vs), 489 (m), 478 (m).

(dppe)Pt{S₂C₂(3-pyridine)(H)} (33) was prepared and isolated as described for **24** using 1-pyridin-3-yl-2-bromoethanone (0.025 g, 0.125 mmol) and (dppe)Pt(SH)₂ (0.066 g, 0.1 mmol). Complex **33** was isolated as a yellow solid in 36% yield (0.027 g, 0.047 mmol). Anal. Calcd for C₃₃H₂₉NP₂PtS₂: C, 52.04; H, 3.81; N, 1.84. Found: C, 51.92; H, 4.11; N, 1.61. ¹H NMR (CDCl₃): δ 8.81 (s, 1H, C₅H₄ N), 8.27 (d, 1H, C₅H₄ N, J_{H-H} = 8 Hz), 7.98 (dd with ¹⁹⁵Pt satellites, 1H, S₂C₂H, J_{P-H} = 8 Hz; J_{P-H} = 1 Hz; J_{Pt-H} = 90 Hz), 7.89–7.80 (m, 8H, PC₆H₅), 7.56–7.48 (m, 12H, PC₆H₅), 7.32 (d, 1H, C₅H₄ N, J_{H-H} = 6 Hz), 7.11 (dd, 1H, C₅H₄ N, J_{H-H} = 8 Hz; J_{H-H} = 6 Hz), 2.59 (m, 2H, PC₂H₂), 2.50 (m, 2H, PC₂H₂). ³¹P NMR (CDCl₃): δ 45.2 (d with Pt satellites, J_{P-P} = 15 Hz; J_{Pt-P} = 2760 Hz), 44.7 (d with Pt satellites, J_{P-P} = 15 Hz; J_{Pt-P} = 2750 Hz). Mass spectrum (FAB) *m/z* = 761 (M⁺), 625 (M⁺ – C₇H₅NS). UV–vis (abs) λ_{max} (ε) (CH₂Cl₂, nm): 314 (4300), 346 (6000), 420 (sh, 460). IR (KBr, cm⁻¹): 3049 (w), 2966 (w), 2920 (w), 1565 (m), 1520 (m), 1490 (m), 1432 (vs), 1406 (w), 1330 (w), 1308 (w), 1270 (w), 1236 (w), 1216 (m), 1185 (m), 1158 (w), 1099 (s), 1026 (m), 998 (m), 910 (m), 878 (m), 818 (m), 747 (m), 719 (s), 705 (s), 698 (vs), 528 (vs), 486 (m).

(dppe)Pt{S₂C₂(4-pyridine)(H)} (34) was prepared and isolated as described for **24** using 1-pyridin-4-yl-2-bromoethanone (0.025 g, 0.125 mmol) and (dppe)Pt(SH)₂ (0.066 g, 0.1 mmol). Complex **34** was isolated as a yellow solid in 38% yield (0.029 g, 0.038 mmol). Anal. Calcd for C₃₃H₂₉NP₂PtS₂: C, 52.04; H, 3.81; N, 1.84. Found: C, 52.41; H, 3.87; N, 1.53. ¹H NMR (CDCl₃): δ 8.33 (d, 2H, C₅H₄ N, J_{H-H} = 6 Hz), 8.00 (d with ¹⁹⁵Pt satellites, 1H, S₂C₂H, J_{P-H} = 8 Hz; J_{Pt-H} = 90 Hz), 7.84–7.79 (m, 8H, PC₆H₅), 7.64 (d, 2H, C₅H₄ N, J_{H-H} = 6 Hz), 7.56–7.47 (m, 12H, PC₆H₅), 2.58 (m, 2H, PC₂H₂), 2.49 (m, 2H, PC₂H₂). ³¹P NMR (CDCl₃): δ 45.4 (d with Pt satellites, J_{P-P} = 14 Hz; J_{Pt-P} = 2770 Hz), 44.9 (d with Pt satellites, J_{P-P} = 14 Hz; J_{Pt-P} = 2750 Hz). Mass spectrum (FAB) *m/z* = 761 (M⁺), 593 (M⁺ – C₇H₅NS₂). UV–vis (abs) λ_{max} (ε) (CH₂Cl₂, nm): 360 (3900), 410 (sh, 560). IR (KBr, cm⁻¹): 3047 (w), 2962 (w), 2919 (w), 1584 (s), 1541 (m), 1506 (s), 1484 (m), 1434 (vs), 1406 (m), 1308 (w), 1263 (w), 1206 (w), 1182 (m), 1150 (w), 1099 (s), 1027 (m), 999 (m), 928 (m), 878 (m), 820 (m), 747 (m), 714 (s), 706 (s), 692 (vs), 528 (vs), 486 (m).

(dppe)Ni{S₂C₂(2-pyrazine)(H)}·CH₂Cl₂ (35) was prepared and isolated as described for **24** using 1-pyrazin-2-yl-2-bromoethanone (0.035 g, 0.174 mmol) and (dppe)Ni(SH)₂ (0.075 g, 0.143 mmol). Complex **35** was isolated as a dark green solid in 54% yield (0.055 g, 0.077 mmol). Analytically pure material was obtained by recrystallization from CH₂Cl₂/pentane. Anal. Calcd for C₃₃H₃₀Cl₂N₂NiP₂S₂: C, 55.80; H, 4.26; N, 3.95. Found: C 55.69; H, 4.20; N, 3.94. ¹H NMR (CDCl₃): δ 8.98 (broad s, 1H, C₄H₃ N₂), 8.32 (broad s, 1H, C₄H₃ N₂), 8.17 (broad s, 1H, C₄H₃ N₂), 7.8–7.7 (m, 9H, PC₆H₅ and S₂C₂H), 7.5–7.4 (m, 12H, PC₆H₅), 2.38 (d, 4H, PC₂H₂, J_{P-H} = 18 Hz). ³¹P NMR (CDCl₃): δ 57.8 (d, second order with line spacing of 8 Hz). Mass spectrum (FAB) *m/z* = 624 (M⁺). UV–vis (abs) λ_{max} (ε) (CH₂Cl₂, nm): 390 (3900), 590 (90). IR (KBr, cm⁻¹): 3053 (w), 2918 (w), 1563 (m), 1496 (s), 1458 (s), 1432 (s), 1382 (w), 1256 (m), 1137 (m), 1101 (s), 1059 (m), 1027 (m), 1010 (m), 991 (m), 877 (m), 817 (m), 749 (m), 713 (sh), 702 (s), 690 (s), 668 (s), 653 (m), 530 (s), 483 (m).

(dppe)Pd{S₂C₂(2-pyrazine)(H)} (36) was prepared and isolated as described for **24** using 1-pyrazin-2-yl-2-bromoethanone (0.036 g, 0.179 mmol) and (dppe)Pd(SH)₂ (0.085 g, 0.149 mmol). Complex **16** was isolated as an orange solid in 52% yield (0.052 g, 0.078 mmol). Anal. Calcd for C₃₂H₂₈N₂P₂PdS₂: C, 57.10; H, 4.19; N, 4.16. Found: C, 56.95; H, 3.87; N, 4.05. ¹H NMR (CDCl₃): δ 8.98 (d, 1H, C₄H₃ N₂, J_{H-H} = 1 Hz), 8.30 (t, 1H, C₄H₃ N₂, J_{H-H} = 1 Hz), 8.17 (d, 1H, C₄H₃ N₂, J_{H-H} = 1 Hz) 7.8–7.7 (m, 9H, PC₆H₅ and S₂C₂H), 7.5–7.4 (m, 12H, PC₆H₅), 2.49 (d, 4H, PC₂H₂, J_{P-H} = 20 Hz). ³¹P NMR (CDCl₃): 47.1 (t, second order with line spacing of 3 Hz). Mass spectrum (FAB) *m/z* = 673 (M⁺). UV–vis (abs) λ_{max} (ε) (CH₂Cl₂, nm): 390 (7500), 520 (80). IR (KBr, cm⁻¹): 3050 (w), 2918 (w), 1566 (s), 1535 (m), 1498 (s), 1457 (s), 1432 (s), 1386 (m), 1257 (m), 1212 (m), 1186 (m), 1138 (m), 1102 (s), 1060 (m), 1024 (m), 1009 (m), 996 (m), 910 (m), 877 (m), 850 (m), 817 (m), 746 (m), 705 (s), 690 (s), 655 (m), 523 (s), 487 (m), 477 (m).

(dppe)Pt{S₂C₂(2-pyrazine)(H)} (37) was prepared and isolated as described for **24** using 1-pyrazin-2-yl-2-bromoethanone (0.080 g, 0.125 mmol) and (dppe)Pt(SH)₂ (0.029 g, 0.146). Complex **37** was isolated as a yellow solid in 48% yield (0.044 g, 0.058 mmol). ¹H NMR (CDCl₃): δ 8.99 (d, 1H, C₄H₃ N₂, J_{H-H} = 1 Hz), 8.35 (t, 1H, C₄H₃ N₂, J_{H-H} = 1 Hz), 8.13 (d, 1H, C₄H₃ N₂, J_{H-H} = 1 Hz), 7.8–7.7 (m, 9H, PC₆H₅ and S₂C₂H), 7.5–7.4 (m, 12H, PC₆H₅), 2.40 (m, 4H, PC₂H₂). ³¹P NMR (CDCl₃): δ 45.4 (d with Pt satellites, J_{P-P} = 14 Hz; J_{Pt-P} = 2771 Hz), 45.1 (d with Pt satellites, J_{P-P} = 15 Hz; J_{Pt-P} = 2735 Hz). Mass spectrum HRMS (FAB) calcd for C₃₂H₂₈N₂P₂PtS₂ *m/z* = 761.083 47, found *m/z* = 761.081 73 (M⁺). UV–vis (abs) λ_{max} (ε) (CH₂Cl₂, nm): 360 (5100), 382 (6800). IR (KBr, cm⁻¹): 3053 (w), 2921 (w), 1669 (s), 1560 (s), 1498 (s), 1458 (s), 1436 (s), 1385 (m), 1259 (w), 1138 (m), 1102 (s), 1060 (m), 1009 (m), 997 (m), 880 (m), 821 (m), 748 (m), 703 (s), 689 (s), 655 (m), 532 (s), 484 (s).

10–23 as the [BF₄]⁻ Salts. HBF₄·OEt₂ (54%) etherate was added dropwise to dichloromethane solutions of the neutral complexes **24–37**, until the UV–visible bands for the neutral complexes were replaced by those of the protonated complexes **10–23**, respectively. The solvent was removed in air, and the solids washed with diethyl ether, 3 × 10 mL. Complexes **10–13** were isolated as purple solids, while **14–23** were isolated as orange solids in ≥95%.

Structural Determination of (dppe)Ni{S₂C₂(2-pyrazine)(H)} (35). Crystal data collection and refinement parameters are collected in Table 1. The data collection was performed on a Siemens P4 equipped with a CCD detector. The systematic absences in the diffraction data are uniquely consistent with the reported space group. The structure was solved using direct methods, completed by subsequent difference Fourier syntheses and refined by full-matrix least squares procedures. All non-hydrogen atoms were refined with anisotropic displacement coefficients, and hydrogen atoms were treated as idealized contributions.

All software and sources of the scattering factors are contained in the SHELXTL (5.3) and SMART program library (Siemens XRD, Madison, WI).

pK_a of 10–12, 16, 19, and 20 in CH₃CN. The pK_a values of **10–12** and **19** were determined by the progressive addition of [pyridinium]-[BPh₄] to CH₃CN solutions of **24–26** and **33**, respectively. The concentrations of the respective neutral and protonated complexes **10–12**, **19**, **24–26**, and **33** were obtained from the UV–visible absorbance of the lowest energy bands at λ_{max}. The pyridinium and pyridine concentrations were determined from the known amount of [pyridinium]-

[BPh₄] added and the concentrations of the protonated and neutral metal complexes. The p*K*_a values for **10**–**12** and **19** were calculated in acetonitrile at five points between 20–80% of the initial concentration of the neutral complexes using eq 2. The p*K*_a' for [pyridinium][BPh₄],

$$pK_a = pK_a' + \log K_{eq} \quad (2)$$

12.3, was obtained from the literature,³⁰ and the *K*_{eq} values were calculated using eq 3, where [X] = [**24**], [**25**], [**26**], or [**33**] while, [XH⁺]

$$K_{eq} = [XH^+]^2 / ([pyridinium]_{added} - [XH^+])[X] \quad (3)$$

= [**10**], [**11**], [**12**], or [**19**], respectively. It was not necessary to consider the formation of [Py–H–Py]⁺ in the p*K*_a calculations since its concentration would impart less than a 1% error to the p*K*_a values of these complexes.³²

The p*K*_a values of complexes **16** and **20** were determined from the addition of 1 equiv of [pyridinium][BPh₄] to **30** and **34** followed by titration with a standardized solution of pyridine. The p*K*_a values were calculated using eq 2 at five points from 20 to 80% of the initial concentration of the neutral complexes. The concentrations of the respective neutral and protonated complexes were obtained from the

UV–visible absorbance of the lowest energy bands at λ_{max}. The pyridinium and pyridine concentrations were determined from the known amounts of these reagents added and the concentrations of the protonated and neutral metal complexes. p*K*_a' was 12.3, the p*K*_a of [pyridinium][BPh₄],³⁰ and the *K*_{eq} values were calculated using eq 4,

$$K_{eq} = [XH^+](\text{[pyridine]}_{added} + \text{[pyridinium]}_{added} - [X]) / [X]^2 \quad (4)$$

where [X] = [**30**] or [**34**] while [XH⁺] = [**16**] or [**20**], respectively. The experiments were repeated three times and the results averaged. The uncertainties reported are the standard deviations of the average p*K*_a values.

Acknowledgment. We are indebted to the Donors of the Petroleum Research Fund, administered by the American Chemical Society (Grants 28499G3 and 3248GAC3), and the Exxon Education Foundation for supporting this research.

Supporting Information Available: An X-ray crystallographic file in CIF format for complex **35** is available on the Internet only. Access information is given on any current masthead page.

IC970194S